

Simulation of (Na-Ta₂O₅) angular interrogation surface plasmon resonance sensor for toluene (C₇H₈) liquids

Farah Jawad Kadhum^{1,*} , Jasim Shamki Alikan¹, Sahar A. Mohammed¹ ,
Ali Abid Dawood Al-Zuky¹ , Anwar Hassn Al- Saleh² 

¹Mustansiriyah University, College of Science, Physics Department, Baghdad, Iraq.

²Mustansiriyah University, College of Science, Department of Computer Science, Baghdad, Iraq.

*Corresponding author: farahjawadalnuaimi@uomustansiriyah.edu.iq

Original Research

Abstract:

Published online:
15 June 2024

© The Author(s) 2024

Surface plasmon resonance (SPR) is a very sensitive technique for keeping track of changes in the optical properties close to the sensor surface. In the Kretschmann configuration, it can be triggered by an evanescent field resulting from total internal reflection from the rear of the sensor surface. The layers were deposited on the semicircular glass prism LASF35 using toluene (C₇H₈) as a sensing medium. The simulation model was created at a sodium (Na) layer thickness of (d_{Na}) (d_{Na} = 50 nm) layers and at varying thicknesses of tantalum pentoxide (Ta₂O₅) (d_{Ta₂O₅}). The parameters of the surface plasmon resonance angle (SPR) were computed. SPR occurred strongly and well in the IR area at (800, 900) nm when it was not seen in the ultraviolet region (100 nm) and appeared in the visible region at 500, 600, and 700 nm. The visible region's highest sensitivity (S = 190) occurred at 700 nm, where the sodium layer thickness (d_{Na}) values of SPR dip length (L_d) and full width half maximum (FWHM) were excellent (50 nm). As a result, the suggested sensor can operate at wavelengths of 500, 600, 700, 800, and 900 nm in the IR-visible range.

Keywords: Surface plasmon resonance; Angular interrogation; Liquid sensor; Theoretical model; Sensitivity

1. Introduction

Conduction electrons oscillate resonantly at the boundary of materials with opposing permittivity's as TM light enters the system, is known as surface plasmon resonance (SPR). Numerous industry-recognized instruments for determining the amount of material that has been absorbed into planar metal surfaces (typically gold Au or silver Ag) or the surfaces with metal particles are based on SPR. This fundamental concept underlies many color-based biosensor applications, including lab-on-a-chip sensors and diatom photosynthesis [1]. The SPR sensor is used in a variety of bio sensing applications to identify, assess, and characterize biomolecules, chemicals, the environment, and food [2]. Additionally, these sensors are very sensitive and enable real-time analyte analysis [3]. This demonstrates a variety of optical features, such as how variations in refractive index (RI) affect the resonance frequency or angle of the sensor layer. The SPR sensor exhibits a dramatic dip in the resonance reflectivity curve at the particular refractive index for

the sensing layer at the resonance [4]. The adsorption of the incoming light in the sensing medium results in a dramatic dip in the resonance curve [5]. The best configuration for designing the sensor is the Kretschmann setup. The kind of sensing medium (liquid or gas) as well as the kind of system design (optical fiber, a prism, and a diffraction grating) have a considerable impact on the sensitivity of SPR measurements [6]. The design or development of using SPR devices like sensors for identify any changes within optical characteristics of the media being investigated is among the most significant simulated and practical studies of the SPR sensor system ever introduced [7]. Demonstrated that the graphene-based SPR bio-sensor sensitivity was greater than the conventional thin gold SPR bio-sensor. Its enhanced sensitivity is due to graphene's greater capacity to absorb biomolecules. While [8] simulated building the SPR bimetallic sensor from a pair of silver and gold, as well as using an air gap layer and an indium phosphide stem coating. The SPR gun phenomenon has been widely

exploited in various analytical research disciplines because of its advantages, such as sensitivity, and it was noted that it appears in the UV region but very sometimes in the visible. A research investigation into a trustworthy multimedia source as coupling prism materials for SPR quantitative response and quick and free detection from the posters, optimally precipitated layers of fossil viscera (silver, Aluminum, and Copper films) on BK7 glass are utilized. They also investigated several reflection spectra and performance factors, and their bio-sensor was capable of sensing 1/1000 of the RIU variant medium. On the basis of side-polished photonic crystal fiber, a very sensitive plasmonic refractive index sensor is explored by [9]. The sensor is easily constructed and reasonably priced. An extra layer of Ta₂O₅ is utilized as a high refractive index (RI) material over the plasmonic Ag layer, and its impact on the sensing properties is carefully investigated. According to the in-depth analysis, The RI range for aqueous media is adjusted from 1.38 – 1.42 to 1.34 – 1.41 when the thickness of Ta₂O₅ is increased of (20 – 40) nm. A very sensitive technique for monitoring changes in optical characteristics close to a sensor's surface is surface plasmon resonance, according to [10]. Using water as the sensing medium, SPR can be used to develop simulation models for layers of titanium oxide and silver that are positioned on the semicircular glass prism D-ZLAF50. SPR appeared significantly in the visible and infrared spectrum, but was not apparent in the ultraviolet spectrum, the visible spectrum exhibits the highest sensitivity ($S = 140$). There is a modeling tool available for computing a multilayer's SPR effect system by [11]. A program called Simulation-SPR studies a prism-based system's reflectance as well as the SPR sensitivity (S) and Full Width Half Maximum (FWHM) of the system. As the resonance curves become more acute, the FWHM gets smaller, and the amount of reflectivity loss gets smaller. The findings show effective change detection in sensitive layer refractive index Δn (0, 0.01, 0.05, and 0.1), and higher sensitivity $S = 134$ was attained at $\Delta n = 0.05$.

In the spectral bands of the proposed sensor model, where electromagnetic waves' ability to reflect in the specified range of 100 – 1000 nm works in sensing pollution in toluene liquid, the goal of this simulation study is to: identify the surface plasmon resonance SPR system a broad spectrum of wavelengths; and identify its incident SPR angle. The system is composed of two layers, the first of which is a layer of sodium (Na) with a thickness of d_{Na} , and the second of which is a layer of tantalum pentoxide (Ta₂O₅) with $d_{Ta_2O_5}$. The layers formed using toluene C₇H₈ as the sensing medium on the semicircular glass prism LASF35. The behavior of the SPR curve is studied by changing the sample thickness and the incident angle for different wavelengths. It gives the sensing range of wavelengths and optimal angles to get a resonant surface plasmon.

2. Theoretical part

The wavelengths of the incident electromagnetic waves correspond the surface electrons' wavelengths when illuminated by p-polarized light, resulting in surface plasmon resonance (SPR), which is regarded as an optical occur-

rence, at the junction of an insulating layer and a metallic surface [12]. In the SPR process, (transverse magnetic) TM or p-polarized light excites electron density oscillations at the metal-dielectric interface, which are referred to as surface plasmon waves, or SPWs. A resonance takes place when the incident light's energy and momentum matches those of the SPW, causing a sudden drop in the intensity of light that is reflected. The light's wavelength beam, the angle of incidence, include the dielectric properties of both the metal and the dielectric all affect the resonance situation. The sharp dip will only emerge at a specific angle if the wavelength is maintained constant and the angle of incidence is changed. This technique is known as "angular interrogation". Another technique, known as spectral or wavelength interrogation, varies the wavelength while varying the incident beam's angle. Resonance happens in this method at a specific wavelength. The refractive index of the dielectric medium affects the resonance parameter's (angle or wavelength) value. The resonance parameter's value changes when the refractive index changes. In most cases, a prism is utilized to stimulate surface plasmons [13]. SPR sensors have received extensive research due to their alluring qualities of accurate estimation, quick responsiveness, immediate detection, and excellent label-free lighting control skills [14]. On noble metallic surfaces like gold and silver, surface plasmon resonance has traditionally been employed to measure medium sensitivity (liquid and gas). These substances (or metals) have a few advantages over other varieties of minerals, including visible and near-infrared SPR bands, well-defined surface chemistry, and the ability to produce films using a variety of deposition techniques [15]. The most popular usage of SPR is in liquid sensing activity, where pollutant molecule attachment results in a slight change in the insulating medium's RI close to the interface that may be picked up by altering the metal surface's reflection [16]. When pollutants adhere to a metal surface, the resonance angle varies according to the optical system analysis concentration. Since they have advantages including sensitivity, detection speed, quantitative response, and label-free detection, SPR sensors have been extensively used in a variety of analytical research fields. Through their interaction with the metallic layer, SPRs disperse their electromagnetic waves [17]. The connection between light and a metal surface. The exceptional sensitivity of SPR to the refractive index of the medium next to the metallic surface makes it useful for sensing applications. SPR occurs at the interface of two mediators. The following dispersion relation is observed for electronic and magnetic surface plasmons [18]:

$$K(w) = \frac{w}{c} \sqrt{\frac{\epsilon_1 \epsilon_2 \mu_1 \mu_2}{\epsilon_1 \mu_1 + \epsilon_2 \mu_2}} \quad (1)$$

Where $K(w)$: is the wave vector, ϵ_1 , ϵ_2 and μ_1 , μ_2 are the relative permittivities and relative permeabilities of glass block and metal film respectively. While c is the speed of light in a vacuum and w is angular frequency. Silver and gold are the most common metals that sustain surface plasmons, however other metals including copper, sodium, titanium, or chromium have also been utilized [18]. The ratio of the electric field of a reflected and transmitted wave to

the electric field of the incoming wave is known as Fresnel's equations. The relative amplitude and phase shifts between waves, as well as the reflection and transmission of light when it strikes an interface between two different media, are all described by these complex ratios [19].

Depending on the angle of incidence, light will reflect and be refracted as it hits an insulating surface. The "law of reflection" and "Snell's law" determine the direction of the refracted and reflected waves. To determine the reflectivity and transmittance coefficients between any two media, the Fresnel equation for TM-polarized light has been used. The two equations for reflectivity coefficient, r_p and transmittance coefficient, t_p were then generalized to determine the overall reflexivity of the proposed system [19]:

$$r_p = \frac{n_2 \cos \theta_i - n_1 \cos \theta_t}{n_2 \cos \theta_i + n_1 \cos \theta_t} \quad (2)$$

$$t_p = \frac{2n_1 \cos \theta_i}{n_2 \cos \theta_i + n_1 \cos \theta_t}$$

n_1 and n_2 are RIs for incident wave media (1) and refractive wave media (2), respectively. Finally, θ_i and θ_t are the incident and the refractive angles, respectively.

3. Experimental work

The newly presented SPR sensor is made up of a glass hemispheric prism of type LASF35, on which two layers - the first of which is a metal Na film and the second of which is a Ta₂O₅ film - have been deposited. Toluene (C₇H₈) is then used as the sensing medium.

The proposed SPR's schematic diagram is shown in Figure 1.

This work used a Kretschmann SPR system configuration and utilized a broad variety of the electromagnetic spectrum, beginning in the IR, visible, and UV regions.

The following list of variables will be modified the simulation's operation algorithm:

- The wavelength range of electromagnetic waves is 100 nm to 1000 nm, with a 100 nm step between ultraviolet and infrared.
- Incident angles of electromagnetic waves (0 – 90°, step

1°).

- Prism LASF35- glass hemircircle of refractive index $n_g(\lambda)$.
- A layer of sodium (Na) with a thickness of $d_1 = 50$ nm and a refractive index of $n_{Na}(\lambda)$ was put on the base of the prism.
- Dielectric tantalum pentoxide (Ta₂O₅) layer thickness $d_2 = (0, 50, 100, 150, 200$ and $250)$ nm step changes 50 nm and refractive index $n_{Ta_2O_5}(\lambda)$ deposited on sodium layer.
- Sensing medium: which consider to be toluene C₇H₈ of refractive index $n_{C_7H_8}(\lambda)$, and the degree of change in the external sensing medium's refractive index that comes into contact with the sensor is ($\Delta n = 0$ and 0.04).

This study presents the outcomes of a simulated surface plasmon resonance SPR sensor incorporating metallic layer, specifically sodium, which is pivotal in inducing the SPR phenomenon. However, due to its reactivity, sodium can potentially interact with the Ta₂O₅ layer, impeding the functionality of the proposed model in practical applications. This challenge can be effectively overcome by the deposition of a thin layer of gold, acting as a barrier to avert any unwanted reactions between sodium and Ta₂O₅. Such an approach allows for the continued operation of the sensor without compromising its performance.

A crucial point to remember is that the refractive indices of the system's components, including the prism LASF35-glass, sodium, toluene, and Ta₂O₅ dielectric, alterations when incident wavelengths alter. These materials' refractive indices were taken from the website (refractiveindex.info) [20]. Figure 2 depicts the relationship between the newly introduced system material's refractive indices (real parts (n) and imaginary parts (k)) and wavelengths (λ) in range of 100 nm to 1000 nm [20]. Refractive index data obtained from the website (refractiveindex.info). The breadth of the reflectance dip is influenced by dissipation in metal brought on by absorption, and this is mostly determined by the imaginary portion of the metal refractive index. At longer wavelengths, the imaginary sections enlarge, causing the dissipation to increase and the dip to widen.

The simulation of the experimental data was achieved using the following algorithm:

Compute FWMH and L_d algorithm

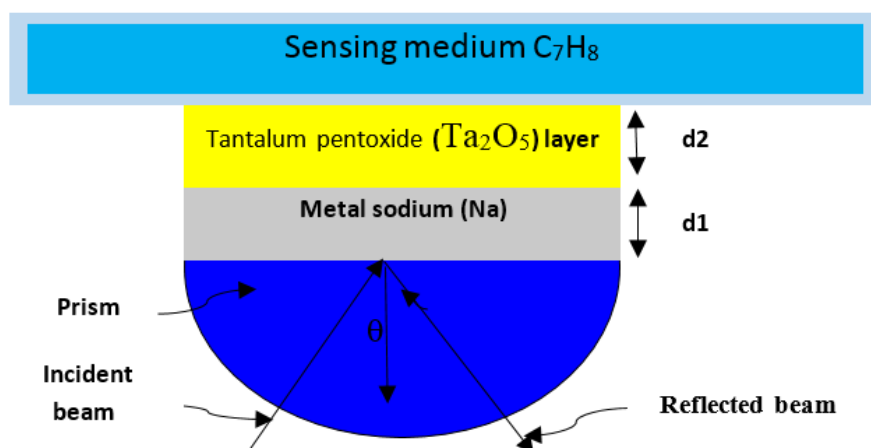


Figure 1. Depicts the toluene SPR sensor's design that has been proposed (glass prism half-sphere).

The dip data represented by $y = f(x)$, where x represents the incident angle (0° to 90°).

Start algorithm

1. Extract maximum SPR peak curve (L_d) at SPR angle ($SPR_{\theta_{theta}}$) using $[L_d \ SPR_{\theta_{theta}}] = \min(y)$
 2. Extract the half max value for the SPR peak curve:
 3. $halfMax = (\min(y) + \max(y)) / 2$;
 4. Extract data at curve decay below halfMax value and save it in halfmax1.
 5. Extract data at curve above halfMax value and save it in halfmax2.
 6. Compute FWHM using $FWMH = halfmax2 - halfmax1$
- End algorithm

4. Results and discussions

By using a MATLAB simulation approach followed by SPR – curve measurements, the performance characteristics of the metal (Na) dielectric and Ta₂O₅ sensor to sense any optical change in toluene have been examined in this work. The reflectance (R) for the Na/Ta₂O₅ structure was developed using a simulation method as a function of incidence angle (θ_i). Figure 3 illustrates a few examples of the Reflectance, Absorbance and transmittance R , A , and T curves according to incidence angles (θ_i) at various wavelengths. Therefore, for the suggested SPR sensor, first determine the

best wavelength for the system’s illumination. It can be seen from this image that the surface plasmon resonance (SPR) occurs when the reflectance curve exhibits a high abrupt dip while also exhibiting the absorption-curve a high sharp peak. Though the transmission curve was not much impacted. In other words, the reflectance curve complements the absorption curve by giving a dramatic peak where the absorption curve exhibits a severe dip and a drastically decreased reflectivity.

- SPR was present in the reflectance and absorbance (R - A) curves but disappeared in the transmittance (T -curve), which remained stable across all thicknesses and wavelengths.
- The SPR angle gradually changed towards higher values when the sensing medium’s refractive index $\Delta n = (0$ and $0.04)$ increased, according to [21]. The complete examples of the R -curves for various Ta₂O₅ layer thicknesses and wavelengths are illustrated in Figure 4. These reflection curves reveal the following:
- The range of wavelengths from 100 to 500 nm does not exhibit SPR.
- At a wavelength of 600 nm, SPR first appears with an incomplete dip.
- The sensor’s resolution degrades at other wavelengths as a result of the reflectance dip’s broadening, and accuracy is

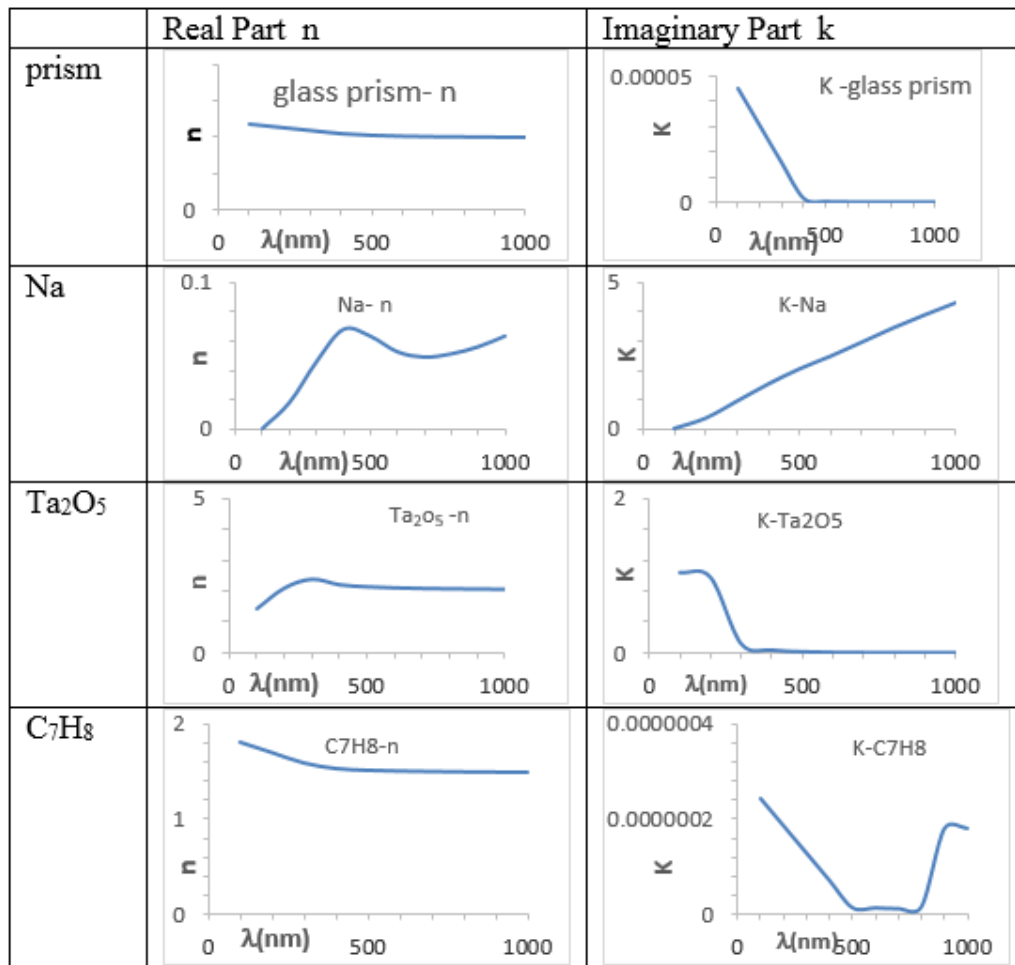


Figure 2. Shows the real and imaginary parts for proposed SPR sensor layers [20].

therefore dependent on the resonance damping's width and shape.

- There is only one thickness connected with a specific SPR detector setup, and at a given wavelength, this enables a perfect energy transfer from the illuminating light to the plasmon wave.

The SPR dip's length is near one, and the reflectance ($R - \theta$) curve for the SPR sensor is developed using a simulation algorithm to provide the smallest feasible FWHM for the SPR dip. The reflectance curves for the Ta₂O₅ layer with varied thickness are shown in Figure 4. The surface plasmon resonance angle θ_i controls it. The largest energy loss from the activation regarding the surface plasmon occurs at the angle of incidence where a small reflection θ_{SPR} happens. The reflectivity curve properties likewise, SPRs may occur. Summed up as follows:

- No states of SPR can be applied during the sensing process.
- With a Ta₂O₅ thickness of 0 – 250 nm. However, SPR states started to develop at wavelengths of 500 nm, improved at 600, 700, 800, and 900 nm, and became faint at 1000 nm.
- SPRs become very strong at thicknesses Ta₂O₅ layer $d_2 = 150$ nm at wavelengths (500 and 600) nm, $d_2 = 200$ nm at wavelength 700 nm and $d_2 = 250$ nm at wavelength 800 nm.

The best SPR sensor has a full-width half maximum

(FWHM) and a height L_d that are closer to one, a sharper FWHM, and a longer L_d , are the properties of the SPR dip for R -curves. Additionally, [22] is used to calculate the sensor sensitivity (S):

$$S = \frac{\Delta\theta_{SPR}}{\Delta n} \tag{3}$$

$\Delta\theta_{SPR}$: measures the size of the angular displacement caused by the surface plasmon resonance dip as a result of a change in the sensing medium's refractive index Δn .

The estimated full-width half maximum (FWHM) and length (L_d) of the SPR dips when the outer medium's refractive index changes are shown in Figure 5 with $\Delta n = 0$ and 0.04, respectively. It should be observed that the SPR dip's FWHM is almost always steady as Ta₂O₅ thickness increases but gradually decreases as wavelengths increase. The analysis of the FWHM values is as follows:

- When used with $d_2 = (100 \& 150)$ nm, the FWHM at $\lambda = 500$ nm has very good values ($1.2^\circ - 3^\circ$).
- Very good FWHM values ($0.8^\circ - 1^\circ$) were obtained at $\lambda = 600$ nm, $d_2 = 150$ nm, and good FWHM values ($2.7^\circ - 3.9^\circ$) were obtained at $d_2 = 200$ nm and 250 nm, respectively.
- At $d_2 = 200$ nm, $\lambda = 700$ nm yields very good FWHM values ($1.1^\circ - 1^\circ$), while $d_2 = 250$ nm yields good values.
- At $d_2 = 250$ nm and $\lambda = 800$ nm, good FWHM values ($1.6^\circ - 1.4^\circ$) are obtained.

In addition, noted that the SPR dip length (L_d) was steady in values smaller than 1 at all Ta₂O₅ thicknesses and that

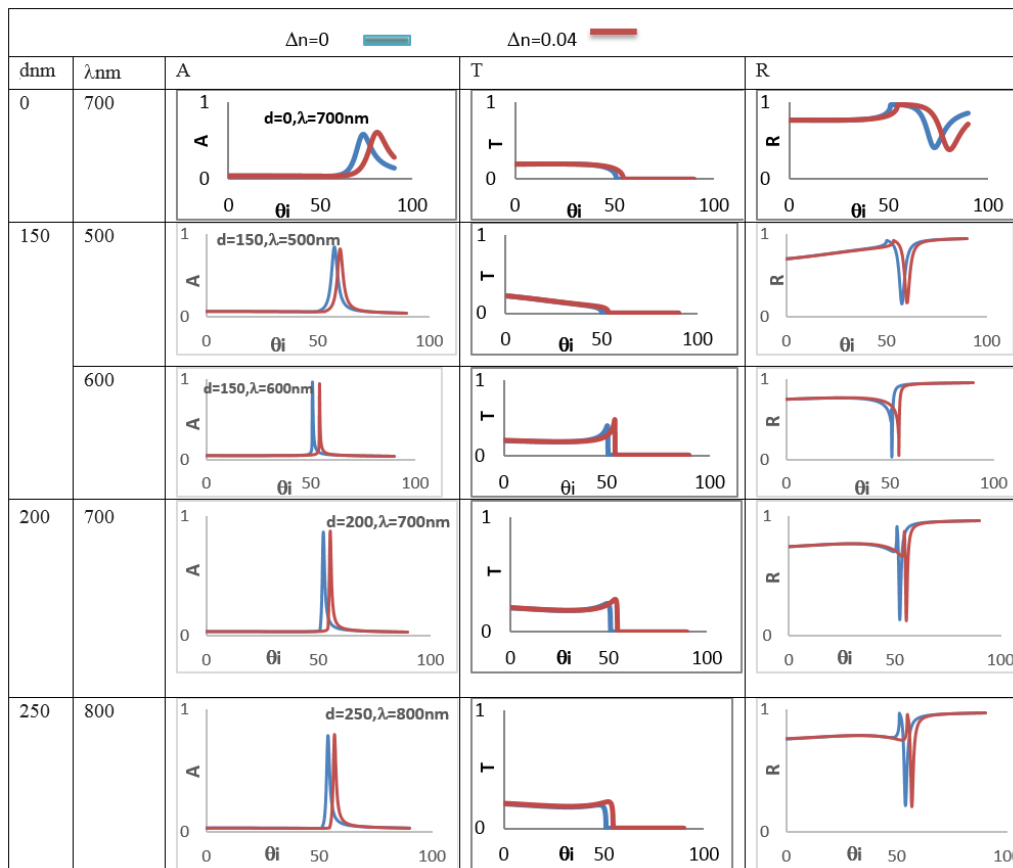


Figure 3. R-A-T curve variations based on incidence angles at various operating wavelengths, with variable Ta₂O₅ layer thicknesses and a fixed Na layer thickness of 50 nm, with the sensing medium's refractive index Δn ($= 0$ and 0.04).

the L_d for wavelengths (600 and 700 nm) was between 0.90 and 0.95.

Following is a study of the SPR dip length L_d values presented in Figure 5:

- Acceptable L_d -values at $\lambda = 500$ nm ($0.77^\circ - 0.79^\circ$) at $d_2 = 150$ nm.
- L_d -values are very good ($0.92^\circ - 0.95^\circ$) at $\lambda = 600$ nm and $d_2 = 150, 200,$ and 250 nm.
- L_d -values are good ($0.84^\circ - 0.9^\circ$) at $\lambda = 700$ nm and $d_2 = 200$ & 250 nm.
- L_d values acceptable at $\lambda = 800$ nm and $d_2 = 250$ nm.

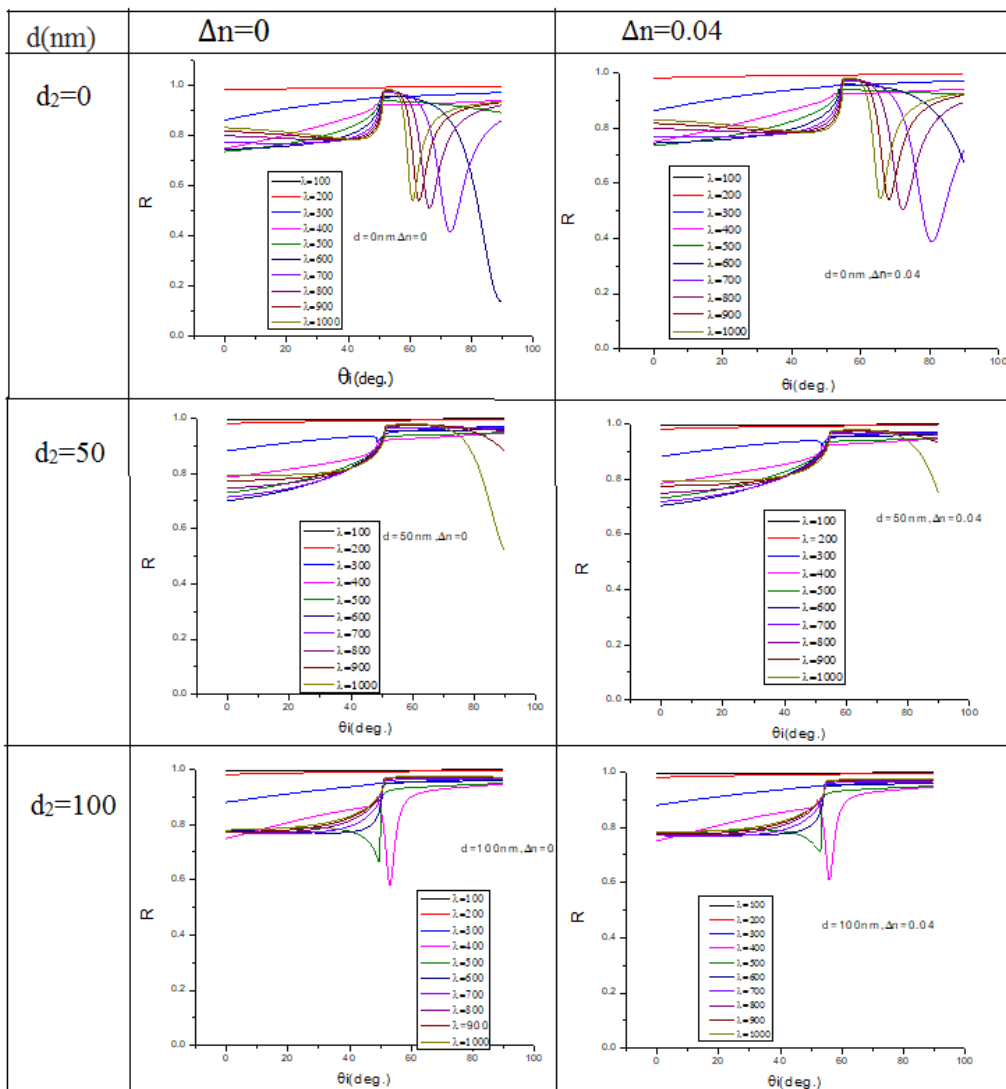
The following can be deduced from L_d and FWHM analysis:

- Acceptable SPR sensor at $\lambda = 500$ nm and $d_2 = 150$ nm.
- A very good SPR sensor worked at $\lambda = 600$ nm & $d_2 = 150$ nm, and a good SPR sensor obtained at $d_2 = (200$ & $250)$ nm.
- At $\lambda = 700$ nm obtained a good SPR sensor at $d_2 = 200$ nm, and acceptable SPR sensor at $d_2 = 250$ nm.
- While at $\lambda = 800$ nm, get an acceptable SPR sensor working at $d_2 = 250$ nm.

The SPR sensor's sensitivity factor (S): is the variation in the SPR sensor's resonance angle (θ_{SPR}) per unit variation in the detecting region's refractive index (Δn) at the sensor surface.

The results of the sensitivity (S) analysis are as follows:

- Sharper dips ($S = 190$) can be used to achieve higher sensitivity (S) in SPR sensors.
- Figure 6 depicts the relationship between sensitivity due to the change in Ta_2O_5 layer thickness and the change in refractive indices of the sensing medium. This relationship is not constant throughout all Ta_2O_5 thickness ranges. However, at 500 and 600 nm, respectively, the sensitivity was at its peak. Additionally, it should be noted that the sensitivity diminishes when measuring the sensing medium's refractive index, Δn , changes more rapidly. The most beneficial sensitivity settings (S) were at 700 nm, where its values ($S = 190$) for thicknesses of 150 nm $d_{Ta_2O_5}$ and $\Delta n = 0.04$ accord with [23].
- At $\lambda = 500$ nm get a good sensitivity values (77.5) at $d_2 = 100$ nm, and acceptable values (40) at $d_2 = 200$ nm.
- At $\lambda = 600$ nm good values obtained (85) at $d_2 = 150$ nm,



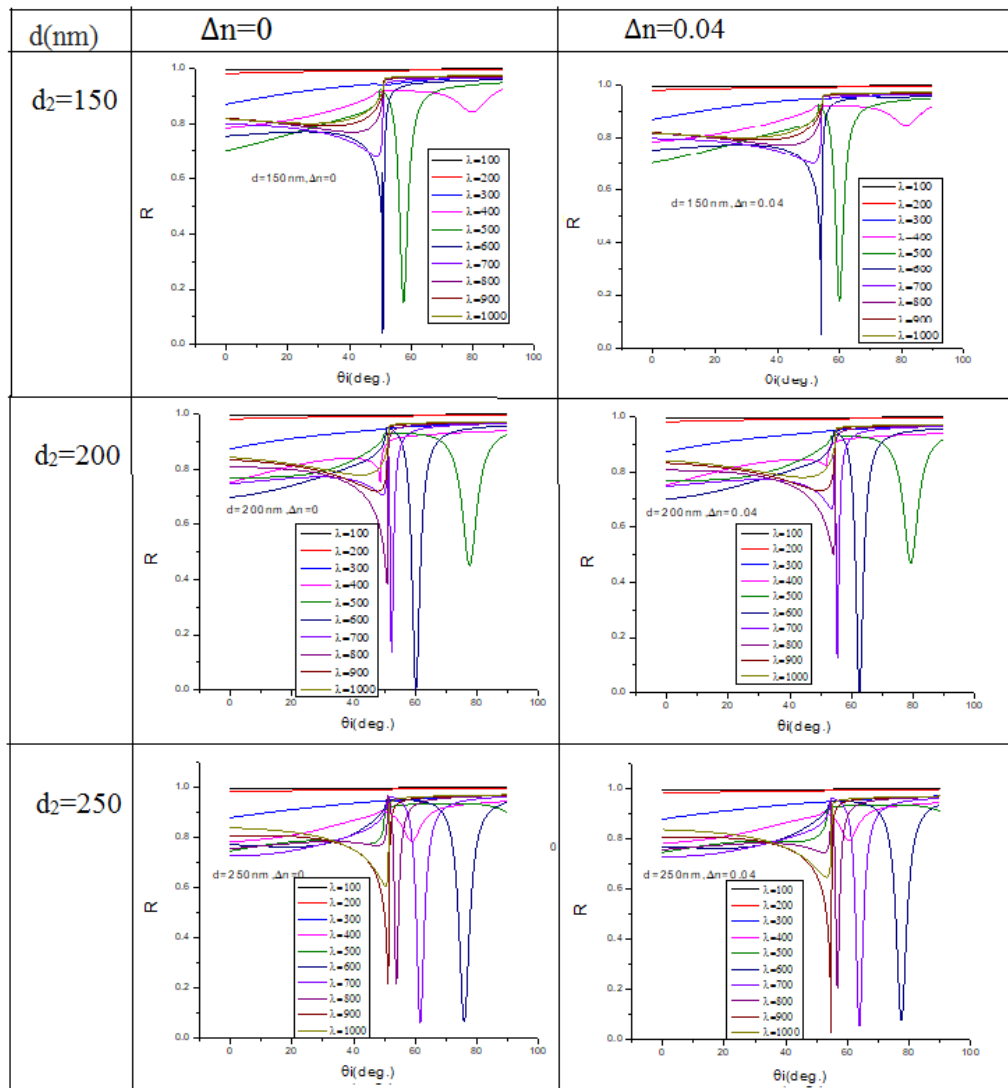


Figure 4. Shows variations in reflectance (R-curves) with varied Ta₂O₅ layer thicknesses and index refraction. It also shows reflectance is a result of incidence angles at various operating wavelengths (λ).

and acceptable values (60 and 40) at $d_2 = 200$ & 250nm.

- At $\lambda = 700$ nm get very good values (190) at $d_2 = 0$ nm, a good values (77.65) at $d_2 = 200$ nm and acceptable values (57.65) at $d_2 = 250$ nm.
- At $\lambda = 800$ nm very good values (147.5) at $d_2 = 0$ nm, and a good values (82.5 and 71.17) at $d_2 = 200$ & 250 nm.
- At $\lambda = 900$ nm very good values (130) at $d_2 = 0$ nm, and good values (87.5) at $d_2 = 250$ nm.

The suggested method can be implemented as a successful system to be used a toluene liquid optical pollution sensor in the IR-visible spectrum at a wavelength of 500 – 900 nm.

5. Conclusion

The results allow for the following conclusions:

1. When the Ta₂O₅ layer is used, the sensitivity (S) increases significantly.
2. The refractive index of the sensing medium varies only slightly when the thickness of the Ta₂O₅ layer, changes and the sensor's dip in reflectance shifts noticeably as a result. This suggests that the resonance angles alter as a result of

the refractive index change.

3. The sensing medium's refractive index rises as a result of a molecular interaction that captures an analyte from the liquid sample in the sensors. The range of the proposed SPR sensor's capacity to recognize minute fluctuations in the target material's index was 0 to 0.04.
4. The SPR phenomenon did not show up within the ultraviolet spectrum, but it did so powerfully in the visible spectrum beginning with a wavelength of 500 nm. It then got even better in the IR spectrum at wavelengths of 800 and 900 nm.
5. The sensor's operating stability was at its highest in the visible spectrum at 500 nm. When used to feel changes in the aqueous medium's refractive index Δn ($= 0 - 0.04$), the sensitivity was attained with values S ($= 190$), the SPR dip length within the ranges of L_d ($\cong 0.90^\circ - 0.95^\circ$), and FWHM ($= 1.2^\circ - 1.6^\circ$), at thicknesses (150, 200, and 250) nm.
6. The full width half maximum (FWHM) and SPR dip length (L_d) values were excellent; the best L_d value was

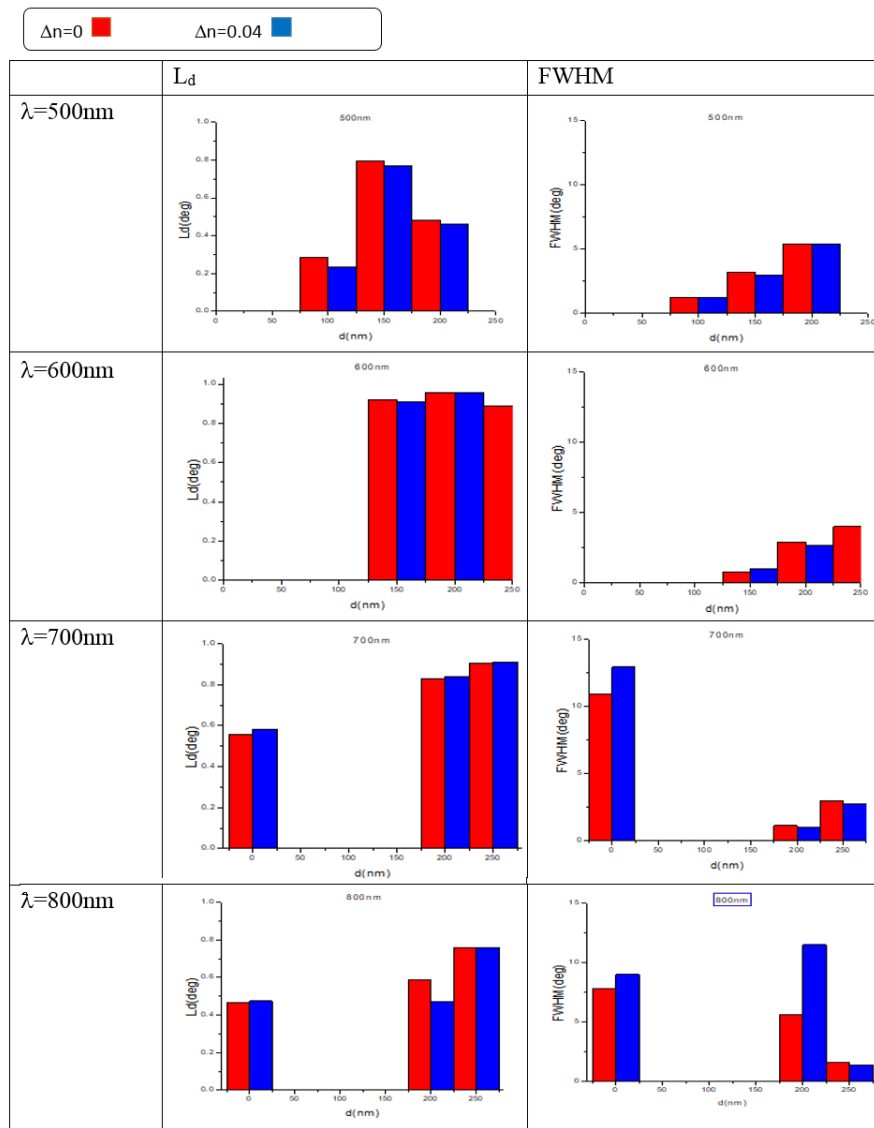


Figure 5. Displays the Full-Width Half Maximum as well as length dip for varied Ta₂O₅ thicknesses and wavelengths with changing layer thin film refractive indices.

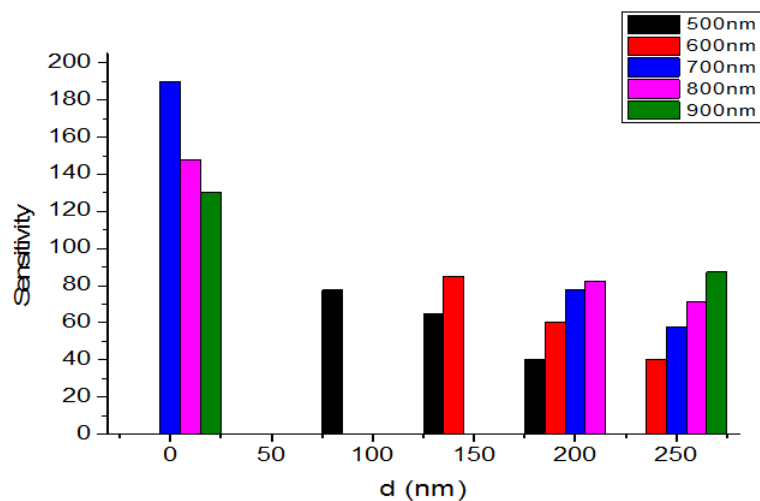


Figure 6. Shows the sensitivity associated with Ta₂O₅ layer thicknesses at various wavelengths with the refractive index Δn .

($\cong 0.90^\circ - 0.95^\circ$); which was for the SPR dip length at the wavelengths of 600 and 700 nm, and $\Delta n = 0.04$.

7. The suggested technology works well as a toluene sensor in the infrared and visible spectrums of wavelengths (500 - 900) nm at the thickness of a Ta₂O₅ layer in the range from (0 to 250) nm.

Acknowledgements

The authors would like to thank Mustansiriyah University (www.uomustansiriyah.edu.iq), Baghdad-Iraq for its support in the present work.

Ethical approval

This manuscript does not report on or involve the use of any animal or human data or tissue. So the ethical approval is not applicable.

Authors Contributions

All the authors have participated sufficiently in the intellectual content, conception and design of this work or the analysis and interpretation of the data (when applicable), as well as the writing of the manuscript.

Availability of data and materials

The datasets generated and analyzed during the current study are available from the corresponding author upon reasonable request.

Conflict of Interests

The author declare that they have no known competing financial interests or personal relationships that could have appeared to influence the work reported in this paper.

Open Access

This article is licensed under a Creative Commons Attribution 4.0 International License, which permits use, sharing, adaptation, distribution and reproduction in any medium or format, as long as you give appropriate credit to the original author(s) and the source, provide a link to the Creative Commons license, and indicate if changes were made. The images or other third party material in this article are included in the article's Creative Commons license, unless indicated otherwise in a credit line to the material. If material is not included in the article's Creative Commons license and your intended use is not permitted by statutory regulation or exceeds the permitted use, you will need to obtain permission directly from the OICCPress publisher. To view a copy of this license, visit <https://creativecommons.org/licenses/by/4.0>.

References

- [1] P. R. Sahoo. "Surface plasmon resonance based biosensor: A new platform for rapid diagnosis of livestock diseases.". *Veterinary World*, **9**:1338–1342, 2016.
- [2] F. Mustafa and S. Andreescu. "Chemical and biological sensors for food-quality monitoring and smart packaging.". *Foods*, **7**:10, 2018.
- [3] A. Srivastava and Y. K. Prajapati. "Performance analysis of silicon and blue phosphorene/MoS₂ heterostructure based SPR sensor.". *Photonic Sensors*, **9**: 284–292, 2019.
- [4] J. Chen. "Optical cavity-enhanced localized surface.". *IEEE Photonics Technology Letters*, **30**:2018–2021, 2018.
- [5] B. Karki. "Sensitivity enhancement of surface plasmon resonance biosensor with 2-D franckeite nanosheets.". *Plasmonics*, **17**:71–78, 2022.
- [6] Q. Wang. "Cu/ITO-coated uncladded fiber-optic biosensor based on surface plasmon resonance.". *IEEE Photonics Technology Letters*, **31**:1159–1162, 2019.
- [7] L. Wu. "Highly sensitive graphene biosensors based on surface plasmon resonance.". *Optics Express*, **18**: 14395, 2010.
- [8] H. K. Rouf and T. Haque. "Performance enhancement of Ag-Au bimetallic surface plasmon resonance biosensor using InP. ". *Progress In Electromagnetics Research M.*, **76**:31–42, 2018.
- [9] S. Das and V. K. Singh. "The role of Ta₂O₅ thin film on a plasmonic refractive index sensor based on photonic crystal fiber. ". *Photonics and Nanostructures - Fundamentals and Applications*, **44**:100904, 2021.
- [10] F. J. Kadhum. "Simulation of surface plasmon resonance (SPR) of silver with titanium oxide as a Bi-layer biosensor.". *Scientific Journal of King Faisal University Basic and Applied Sciences*, **22**:76–80, 2021.
- [11] F. J. Kadhum. "Simulation of surface plasmon resonance (SPR) layers of gold with silicon nitride as a Bi-layer biosensor. ". *Digest Journal of Nanomaterials and Biostructures*, **17**:623–633, 2022.
- [12] G. X. Du. "Evidence of localized surface plasmon enhanced magneto-optical effect in nanodisk array. ". *Applied Physics Letters*, **96**:2008–2011, 2010.
- [13] B. D. Gupta and R. K. Verma. "Surface plasmon resonance-based fiber optic sensors: Principle, probe designs, and some applications.". *Journal of Sensors*, **9**:2009, 2009.
- [14] M. Rosmiza, A. H. Zainul, and W. Mahmood Mat Yunus. "Z. A. T. Multilayers analysis using the phenomenon of surface plasmon resonance.". **28**:83–92, 2007.

- [15] P. Englebienne, A. Hoonacker, M. Van, and Verhas. “Surface plasmon resonance: principles, methods and applications in biomedical sciences. ”. *Spectroscopy*, **17**:372913, 2003.
- [16] W. M. Mukhtar. “Angle shifting in surface plasmon resonance: Experimental and theoretical verification.”. *Journal of Physics: Conference Series*, **431**:1, 2013.
- [17] S. Benaziez, Z. Dibi, and N. Benaziez. “Reflectivity optimization of the SPR graphene sensor. ”. *Nanopages*, **13**:5–17, 2018.
- [18] H. R. Gwon and S. H. Lee. “Spectral and angular responses of surface plasmon resonance based on the kretschmann prism configuration. ”. *Materials Transactions*, **51**:1150–1155, 2010.
- [19] T. Špringer. “Enhancing sensitivity of surface plasmon resonance biosensors by functionalized gold nanoparticles: Size matters. ”. *Analytical Chemistry*, **86**:10350–10356, 2014.
- [20] SCHOTT. “optical glass data sheets.”. , 2012.
- [21] C. L. Giles and W. J. Wild. “Fresnel reflection and transmission at a planar boundary from media of equal refractive indices.”. *Applied Physics Letters*, **40**:210–212, 1982.
- [22] Y. Deng and G. Liu. “Surface plasmons resonance detection based on the attenuated total reflection geometry. ”. *Procedia Engineering*, **7**:432–435, 2010.
- [23] M. Seo, J. Lee, and M. Lee. “Grating-coupled surface plasmon resonance on bulk stainless steel.”. *Optics Express*, **25**:26939, 2017.